RAA 2015 Vol. **15** No. **5**, 651–662 doi: 10.1088/1674–4527/15/5/004
http://www.raa-journal.org *http://www.iop.org/journals/raa*

***R**esearch in*
***A**stronomy and*
***A**strophysics*

The fundamental plane relation of early-type galaxies: environmental dependence

Lei Hou and Yu Wang

Department of Astronomy, University of Science and Technology of China, Hefei 230026, China; *houleihl@mail.ustc.edu.cn*

Received 2014 April 16; accepted 2014 August 14

Abstract Using a sample of 70 793 early-type galaxies from SDSS DR7, we study the environmental dependence of the fundamental plane relation. With the help of the galaxy group catalog based on SDSS DR7, we calculate the fundamental planes in different dark matter halo mass bins for both central and satellite galaxies. We find the environmental dependence of the fundamental plane coefficients is similar in the g, r, i and z bands. The environmental dependence for central and satellite galaxies is significantly different. Although the fundamental plane coefficients for centrals vary systematically with the halo mass, those of satellites are similar in different halo mass bins. The discrepancy between centrals and satellites is significant in small halos, but negligible in the largest halo mass bins. These results remain the same when we only keep red galaxies, or galaxies with $b/a > 0.6$, or galaxies in a specific radius range in the sample. After the correction for the sky background, the results are still similar. We suggest that the different environmental effects of the halo mass on centrals and satellites may arise from their different quenching processes.

Key words: galaxies: elliptical and lenticular — galaxies: halo — galaxies: statistics

1 INTRODUCTION

Galaxies obey several scaling relations between their dynamical and photometric properties. The Tully-Fisher relation Tully & Fisher (1977) shows that brighter spiral galaxies prefer to have larger rotation velocities. For early-type galaxies (elliptical and lenticular galaxies, hereafter ETGs), velocity dispersion is correlated with both luminosity (the Faber-Jackson relation, Faber & Jackson 1976) and the diameter in which the average surface brightness equals a specified value (the $D_n - \sigma$ relation, Dressler et al. 1987). Moreover, there is a scaling relation between these three parameters: central velocity dispersion σ_0, effective radius R_0 and I_0, which is the average surface brightness in R_0 (Djorgovski & Davis 1987; Dressler et al. 1987). This relation is called the fundamental plane (hereafter FP) and is expressed as

$$\log R_0 = a \log \sigma_0 + b \log I_0 + c\,. \tag{1}$$

Both the Faber-Jackson relation and the $D_n - \sigma$ relation can be regarded as projections of the FP relation.

The FP relation reveals a lot of information about the dynamical properties of ETGs. In theory, the properties related to virial equilibrium are expected to give an FP with $a = 2$ and $b = -1$. However, the coefficients of the observed FP relation deviate from this result, a phenomenon which is called the tilt of the FP. Moreover, it is remarkable that the uncertainty in the observed FP is very small, which amounts to a scatter in R_0 of about 20%. Both the tilt and tightness of the FP provide strong constraints on the formation and evolution of ETGs.

Due to the tremendous development in galaxy redshift surveys in recent years, many studies have focused on the FP relation of large samples. Some authors have suggested that the FP is not a universal relation for all ETGs but rather is affected by properties of ETGs. For example, coefficients and residuals associated with FP are correlated with luminosity, magnitude range, Sérsic index, ellipticity, stellar mass-to-light ratio and color (e.g. D'Onofrio et al. 2008; Nigoche-Netro et al. 2009; Magoulas et al. 2012; D'Onofrio et al. 2013). Some studies have also found a systematic variation in stellar population parameters among the different positions on the FP (Graves 2009; La Barbera et al. 2010a; Springob et al. 2012).

Another interesting property of the FP is its environmental dependence. Although some studies declared there is no environmental dependence for the FP (Jorgensen et al. 1996; Reda et al. 2005), others demonstrated the FP coefficients are significantly different between cluster and field ETGs, and between different clusters (Lucey et al. 1991; de Carvalho & Djorgovski 1992; Cappellari et al. 2013). The FP relation is also correlated with dark matter halo mass, richness of a cluster, cluster-centric distance, the distance to the Nth nearest neighbor and local galaxy density (Bernardi et al. 2003c, 2006; D'Onofrio et al. 2008; La Barbera et al. 2010b; Magoulas et al. 2012). However, there is an important problem in these studies: different environmental indicators are adopted. As a result, these studies focused on different aspects of the environmental effects, so it is difficult to directly compare the results of these studies.

In standard ΛCDM cosmology, galaxies are born and located in dark matter halos. The photometric and dynamical properties of galaxies strongly depend on their host halo. The connection between galaxies and halos has been analyzed with models such as the conditional luminosity function (Yang et al. 2003) and halo occupation distribution (Jing et al. 1998; Peacock & Smith 2000). One popular environmental indicator is the mass of the host halo. For example, in larger halos, galaxies are preferentially more massive and redder. Recently, many models prefer to distinguish whether the galaxy is a central or satellite one in the halo. Centrals show a strong correlation to halo mass, but satellites are affected by their accretion history (Yang et al. 2012; Moster et al. 2013). The distinction between centrals and satellites indicates that the position of the galaxy in the halo is another important environmental indicator.

In this work, we adopt the host halo mass and the position of the galaxy in the halo as environmental indicators, and investigate the environmental dependence of the FP relation. With the help of the group catalog based on the Sloan Digital Sky Survey Data Release 7, hereafter SDSS DR7, we get the host halo and derive the mass of the halo for each galaxy in this catalog. Furthermore, we can recognize whether it is a central or satellite galaxy in the halo. Using these two environmental indicators, we investigate the correlation between the environment and the FP coefficients of SDSS ETGs.

The paper is organized as follows. Section 2 describes the sample of ETG data from SDSS DR7, the calculation and corrections of the parameters, and the group catalog which we use to characterize the environment of ETGs. In Section 3, we discuss the virial equilibrium of galaxies in dark matter halos, the fitting method of the FP, the results of the environmental dependence of the FP, and test how systematics are related to the color and axial ratio. We summarize this paper and discuss our findings in Section 4.

We adopt a ΛCDM cosmology with $\Omega_m = 0.238$, $\Omega_\Lambda = 0.762$ and $h = 0.73$ in this work.

2 GALAXY AND GROUP SAMPLES

2.1 Selecting Early-Type Galaxies

This work is based on the data from SDSS DR7[1]. We select ETGs using the following criteria, which are similar to those in Bernardi et al. (2003a):

(1) Concentration r_{90}/r_{50} in the i band is larger than 2.5.
(2) Ratio of the likelihood of the de Vaucouleurs model to the exponential model $L_{\rm deV}/L_{\rm exp} \geq 1.03$.
(3) Spectral classification index *eClass* is less than -0.1.
(4) Warning flag *zWarning* is zero. This is the indicator of high spectral quality.
(5) Signal-to-noise ratio S/N> 10.
(6) Redshift $z < 0.2$. This criterion is the same as in the SDSS group catalog.
(7) Central velocity dispersion $\sigma > 70$ km s^{-1}. This is because the measure of σ lower than this value indicates significant uncertainty.

The number of galaxies in this ETG sample is 70 793.

To measure the FP, we should calculate the radius, the surface brightness and the velocity dispersion of these ETGs. The effective angular radius is

$$r_0 = \sqrt{b/a}\, r_{\rm deV}\,, \tag{2}$$

where b/a is the axial ratio and $r_{\rm deV}$ is the de Vaucouleurs angular radius. Given the redshift of this galaxy, we can convert the effective angular radius into the effective physical radius

$$R_0 = r_0 D_A(z)\,, \tag{3}$$

where $D_A(z)$ is the angular distance at redshift z.

The mean surface brightness in R_0 is defined as $I_0 = L/2R_0^2$. In this work, instead of measuring I_0 directly, we calculate the effective surface brightness $\mu_0 \equiv -2.5\log_{10} I_0$, which is

$$\mu_0 = m_{\rm deV} + 2.5\log_{10}(2\pi r_0^2) - K(z) - 10\log_{10}(1+z) + Qz\,, \tag{4}$$

where $m_{\rm deV}$ is the extinction-corrected de Vaucouleurs magnitude, $K(z)$ is the K-correction to $z = 0$ and Q represents the correction factor for the effect of evolution in luminosity. We use IDL code *kcorrect* v4_2 [2] (Blanton & Roweis 2007) to calculate $K(z)$. Values of Q are taken from Bernardi et al. (2003b).

The central velocity dispersion σ of an SDSS galaxy is estimated from the spectrum, which is observed using a fixed fiber aperture with an angular radius of $1.5''$. As a result, σ of a galaxy with a larger angular radius represents the motion of the more inner stars compared to another galaxy with a smaller radius (Jorgensen et al. 1995; Wegner et al. 1999). We should do an aperture correction as

$$\sigma_0 = \sigma\left(\frac{r_{\rm fiber}}{r_0/8}\right)^{0.04}\,, \tag{5}$$

where $r_{\rm fiber}$ is the angular radius of the fiber and r_0 is the effective radius calculated above.

[1] *http://cas.sdss.org/dr7/en/*
[2] *http://howdy.physics.nyu.edu/index.php/Kcorrect*

2.2 The SDSS Group Catalog

The group catalog is constructed based on SDSS DR7 data using a modified version of the halo-based group finder developed in Yang et al. (2005). This catalog is described in Yang et al. (2007). For each group in the catalog, the dark matter halo mass $M_{\rm halo}$ is estimated by two methods: $M_{\rm L}$, using the characteristic luminosity, and $M_{\rm S}$, using the characteristic stellar mass. In each group, the brightest galaxy is recognized as the central galaxy, and the others are satellites of this group.

Making use of the SDSS group catalog, for each galaxy in the ETG sample, we find its host dark matter halo and the halo mass. Because $M_{\rm halo}$ is more correlated to the stellar mass than to the luminosity, we adopt $M_{\rm S}$ as the estimation of the halo mass in this work. This approach can differentiate whether the galaxy is a central or satellite galaxy. Utilizing the halo mass and the position in the halo as environmental parameters, we can study the environmental dependence of the FP relation in Section 3.3.

3 THE FUNDAMENTAL PLANE RELATION OF EARLY-TYPE GALAXIES

3.1 Galaxies in Virial Equilibrium

According to the virial theorem, galaxies in virial equilibrium should satisfy

$$\sigma^2 \propto \frac{GM}{R} \propto \frac{M}{L} RI\,. \tag{6}$$

If all the ETGs have the same M/L, the FP should satisfy $a = 2$ and $b = -1$. The tilt of the FP occurs when M/L is not constant but rather a function of R, σ or I. The variation of M/L is due to the contribution of non-homology and different stellar populations.

Moreover, the dynamical properties of galaxies are strongly affected by the dark matter halo. Firstly, the dark matter halo provides a potential well in which the stars and gas are located. In addition, tidal effects are exerted on satellite galaxies, which makes the stars and gas in them more easily stripped. By considering the influence of the dark matter, the dynamical equilibrium of ETGs leads to the relation

$$\sigma^2 \propto \frac{GM}{R} + U_m\,, \tag{7}$$

where U_m represents the potential due to the dark matter halo. As a result, the tilt of the FP is correlated with dark matter halos.

Which of these factors plays the most important role in the tilt of the FP? This is a fairly controversial issue (Treu & Koopmans 2004; Rusin & Kochanek 2005; Koopmans et al. 2006; Cappellari et al. 2006; Treu et al. 2006; Bolton et al. 2007, 2008). Recent studies suggest non-homology, differing stellar populations and dark matter all contribute to the tilt. This is called the "hybrid solution" (Trujillo et al. 2004; Hyde & Bernardi 2009; D'Onofrio et al. 2013).

3.2 The FP Relation

After the parameters R_0, μ_0 and σ_0 have been calculated and corrected, we can fit the FP of the ETG sample. There are two methods that can be used to do this task. The direct fit minimizes the scatter in the R_0 direction, while the orthogonal fit minimizes the scatter in the direction orthogonal to the FP. Because the orthogonal fit treats the variables symmetrically, it is thought to be more physically realistic than the direct fit. We adopt the orthogonal fit in this work.

First we calculate the covariance matrix of $I \equiv \log_{10} I_0$, $R \equiv \log_{10} R_0$ and $V \equiv \log_{10} \sigma_0$ of the ETG sample. We should subtract the error matrix from it to get the intrinsic covariance matrix (see

appendix D of Bernardi et al. (2003a) for details)

$$\mathcal{C} \equiv \begin{pmatrix} C_{II} & C_{IR} & C_{IV} \\ C_{IR} & C_{RR} & C_{RV} \\ C_{IV} & C_{RV} & C_{VV} \end{pmatrix}. \tag{8}$$

Then we diagonalize $\mathcal{C}$ and produce the eigenvectors and eigenvalues. Like principal component analysis, the eigenvectors represent the major axes of ETGs in (I, R, V) space, and the eigenvalues are variances in the directions of these three axes. The eigenvector corresponding to the smallest eigenvalue is the normal vector of FP. We can derive FP slopes a and b from the normal vector. The intercept is determined as $c = \overline{R} - a\overline{V} - b\overline{I}$. The uncertainties in a, b and c are measured from 100 repeated bootstrap samples. FP coefficients from our ETG sample are shown in Table 1.

Table 1 FP Fittings for Our ETG Sample

Band (1)	a (2)	b (3)	c (4)	$\mathrm{Scatter}_{\mathrm{orth}}$ (5)	$\mathrm{Scatter}_{R_0}$ (6)
g	1.337 ± 0.004	-0.751 ± 0.001	-8.52 ± 0.01	0.053	0.098
r	1.373 ± 0.004	-0.764 ± 0.001	-8.45 ± 0.01	0.051	0.096
i	1.391 ± 0.004	-0.776 ± 0.001	-8.47 ± 0.01	0.049	0.093
z	1.427 ± 0.004	-0.791 ± 0.002	-8.57 ± 0.01	0.049	0.093

Notes: FP fitting results in the g, r, i and z bands of our ETG sample. Cols. (2) to (4) are a, b and c respectively. Cols. (5) and (6) are scatters in the orthogonal direction and in the R_0 direction respectively.

3.3 Environmental Dependence

As mentioned above, several definitions are used to describe the environment of galaxies, such as centric distance in the group, group richness and local galaxy density. In this work, we make use of the SDSS group catalog and adopt environmental indicators as the mass of the halo and the position in the halo. The advantage of this definition is the understandable connection between galaxies and dark matter halos. In theory, galaxies formed from gaseous halos, and thus show a strong correlation with the dark matter halos. In observations, color, morphology, 2-point correlation function, luminosity function and star formation history depend on the halo mass (e.g. Weinmann et al. 2006; Yang et al. 2012; Woo et al. 2013). Moreover, dark matter halos affect centrals and satellites in distinct ways. Galaxies became satellites when they were accreted into a larger halo, with their star formation easily quenched due to strangulation. Meanwhile, the central galaxy is still accreting gas or merging with other galaxies (van den Bosch et al. 2008; Wetzel et al. 2013). As a result, it is convenient to separate centrals from satellites when considering the environmental dependence.

Depending on the halo mass and the position in the halo, we divide the ETG sample into several subsamples. ETGs with halo mass between $10^{12.0} M_\odot$ and $10^{14.0} M_\odot$ are assigned into eight halo mass bins. The size of each bin is 0.25 order of magnitude. ETGs in halos larger than $10^{14.0} M_\odot$ are placed in a uniform bin. ETGs with halo mass lower than $10^{12.0} M_\odot$ are discarded because the number of them is quite small and the uncertainty is large. In each bin, we separate ETGs into centrals and satellites. These subsamples are shown in Table 2.

FPs of these subsamples are calculated using the above fitting method. We find FPs of all the subsamples are well-shaped and tight. We show projected FPs of subsamples in Figures 1 and 2 for centrals and satellites respectively. In each figure, we only illustrate the shape of FPs in four halo mass bins as examples. The units of σ_0, μ_0 and R_0 are $\mathrm{km\ s^{-1}}$, $\mathrm{mag\ arcsec^{-2}}$ and h^{-1} kpc, respectively. We plot the environmental dependence of FP coefficients in Figure 3.

Several results are indicated in Figure 3. Firstly, FP coefficients as functions of the halo mass are similar in different bands. Secondly, all the FP coefficients of satellites are independent of the

Table 2 Numbers of Centrals and Satellites in Each Halo Mass Bin

$\log M_{\rm halo}$	Centrals	Satellites
$(12.00, 12.25]$	9395	241
$(12.25, 12.50]$	9213	528
$(12.50, 12.75]$	8104	936
$(12.75, 13.00]$	5779	1396
$(13.00, 13.25]$	3848	1858
$(13.25, 13.50]$	2448	2345
$(13.50, 13.75]$	1459	2966
$(13.75, 14.00]$	742	2954
$(14.00, \infty)$	475	6565

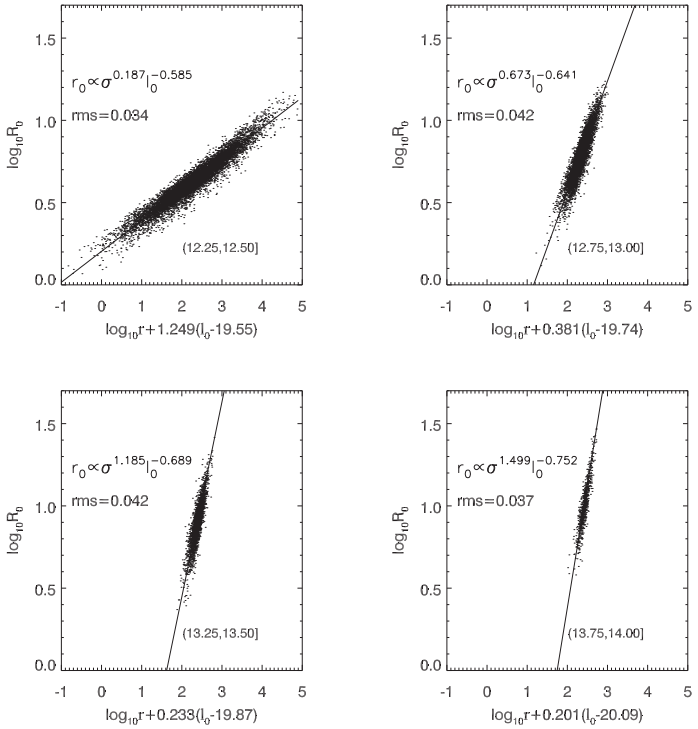

Fig. 1 Projected FPs of centrals in four halo mass bins in the r band. In each subsample, dots represent ETGs and the slope of the solid line represents coefficient a of the FP.

host halo mass and are close to those of the complete ETG sample. Finally, for centrals, we find obvious correlations between FP coefficients and the halo mass. When the halo mass is increasing, a is increasing but b and c are decreasing. In small halos, FP coefficients of centrals are significantly different from those of satellites. In the halos which are more massive than $10^{13.25}\ M_{\odot}$, FP coefficients of centrals only weakly depend on the halo mass, and are close to those of satellites.

The distinction between the environmental dependence of centrals and satellites in Figure 3 is noteworthy. This suggests that satellites form a relatively universal population but centrals do not. In small halos, there is a significant discrepancy between the environment of centrals and satellites. In large halos, the environment of centrals is similar to that of satellites.

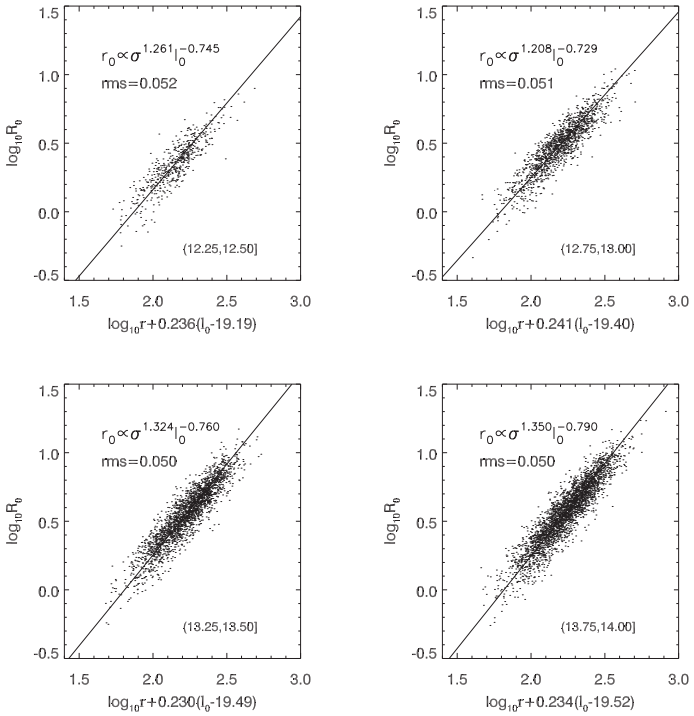

Fig. 2 Projected FPs of satellites in four halo mass bins in the r band. Symbols are the same as in Fig. 1.

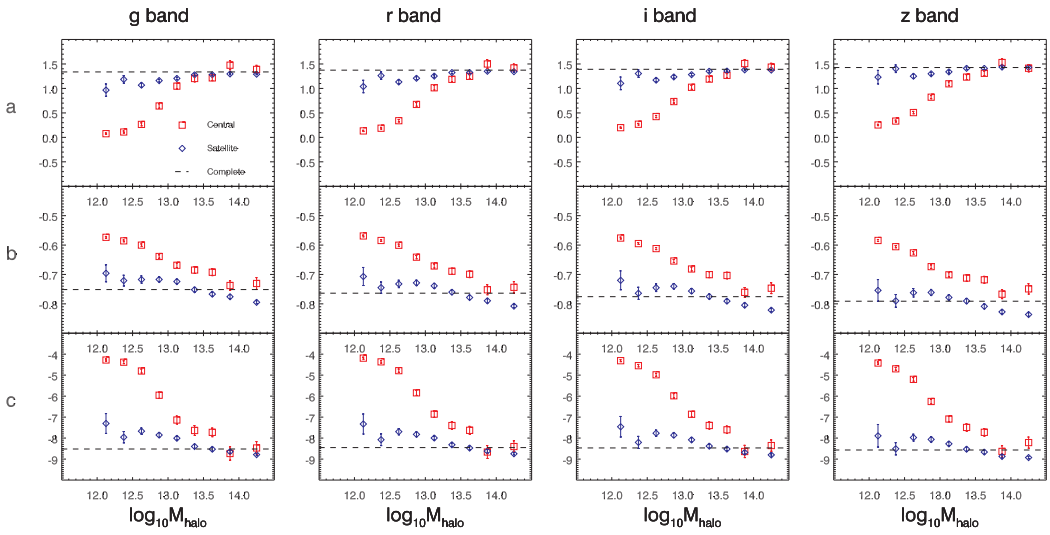

Fig. 3 The environmental dependence of the FP relation in four bands. Red squares are centrals and blue diamonds are satellites. For each subsample, the value of $\log_{10} M_{\rm halo}$ is set as the midpoint of the corresponding halo mass bin. In the last halo mass bin $(14.00, \infty)$, $\log_{10} M_{\rm halo}$ is set as 14.25. The horizontal dashed lines are the corresponding coefficients for the complete ETG sample.

3.4 Systematics

The selection criteria in Section 2.1 do not contain the color constraint or axial ratio constraint. There may be some late-type galaxies included in our sample. The fraction of late-type galaxies increases with decreasing galaxy density, which means there is a larger proportion of late-type galaxies in small halos. We should test whether the environmental dependence of the FP is due to contamination of late-type galaxies.

To do this, all the galaxies in the SDSS DR7 are divided into 120 luminosity bins in such a way that in each bin, there are the same number of galaxies. In each bin, we fit the $g-r$ color distribution of galaxies to a double Gaussian, get the $g-r$ values of the red peak and the blue peak, and calculate the average color of these two peaks. Then a linear fitting is done between the average colors and the average magnitudes in these bins. We find the fitting result is $g-r = 0.68 - 0.030(M_r + 21)$, and adopt this as the dividing line between red and blue galaxies: galaxies above this line are identified as red ones and the others are blue ones. For each subsample in Table 2, we discard blue galaxies to get a corresponding red subsample, and measure its FP relation. FP coefficients of the red subsamples are plotted in Figure 4. We find the dependence of red ETGs is akin to that shown in Figure 3.

Similarly, we can select ETGs with the axial selection criterion. For each subsample in Table 2, we only keep the galaxies with axial ratio $b/a > 0.6$, and measure the FP of the remaining galaxies. As is shown in Figure 5, the environmental dependence of FPs for these galaxies is also akin to that shown in Figure 3.

For a given halo mass bin, centrals and satellites have different stellar mass distributions, especially for the low halo mass bins (Yang et al. 2012). This may bias the FP fitting. Many works indicate that there is a correlation between the size and the stellar mass of galaxies (Trujillo et al. 2006; Cimatti et al. 2008; van Dokkum et al. 2008; Bruce et al. 2012; Bernardi et al. 2014). Therefore, if we force centrals and satellites to have similar $\log R_0$ distributions, to first order, galaxies would have similar stellar mass distributions. This ensures that the FP fittings are compared in a fair and unbiased way. To do this, we fit the $\log R_0$ distribution of ETGs in each halo mass bin to the double Gaussian. Assuming the fitted peaks and standard deviations are μ_1, σ_1, μ_2 and σ_1, with $\mu_1 < \mu_2$, we only keep the galaxies with $\log R_0$ in the range $[\mu_1 - \sigma_1, \mu_2 + \sigma_1]$, and calculate the environmental dependence of the remaining subsamples. We find the result is consistent with Figure 3.

In summary, after performing the color selection, axial ratio selection and radius selection, our results in Figure 3 still remain. This demonstrates the environmental dependence of the FP relation is not due to contamination from late-type galaxies.

Recently, several works indicated that the sky subtraction algorithm used in SDSS DR7 systematically overestimates the sky background of large galaxies and galaxies in dense regions. Therefore, the surface brightness and the half-light radii of centrals are underestimated (Bernardi et al. 2007; Lauer et al. 2007; von der Linden et al. 2007; He et al. 2013; Aihara et al. 2011). It has been suggested that the sky background should be estimated using the global sky in the field rather than the local sky that is adopted in the SDSS pipeline. To test whether this results in a bias in the FP, we corrected this bias as

$$I_{0\mathrm{corr}} = I_0 + I_{\mathrm{LocalSky}} - I_{\mathrm{GlobalSky}}, \tag{9}$$

and re-fit the FPs. FP fitting results of the ETG sample with sky background correction are shown in Table 3, which are similar to those in Table 1. We also find that the sky background correction does not affect the environmental dependence of FP coefficients. Moreover, we also analyze the effect of the bias on the galaxy size. The effective sizes of centrals are underestimated, and this bias is more significant for larger centrals (Aihara et al. 2011). Conjecturing that $\log R_0$ is more underestimated at the large $\log R_0$ end of the FP, we can qualitatively find this makes coefficient a lower and coefficient b higher. Meanwhile, this bias is more significant for centrals in larger halos. Therefore, for centrals in larger halos, coefficient a should receive a more positive correction and coefficient b should receive a more negative correction. This would strengthen the environmental

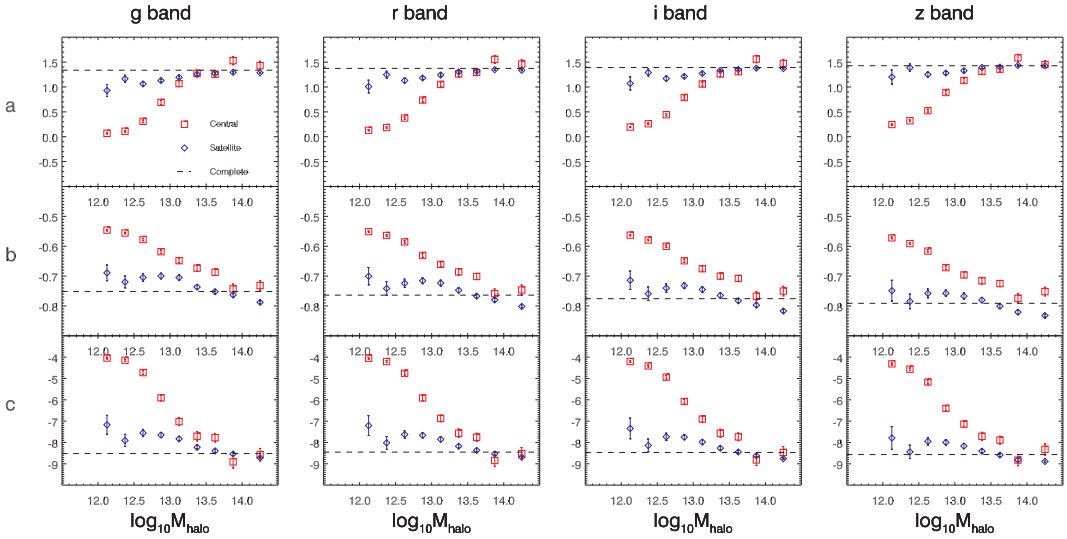

Fig. 4 Environmental dependence of FP coefficients for red ETGs. Symbols are the same as in Fig. 3.

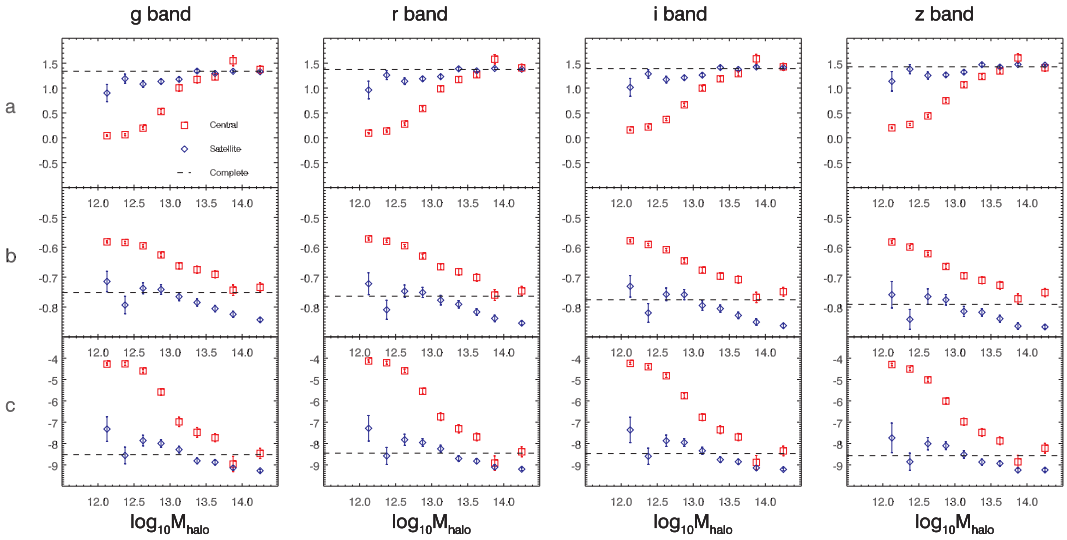

Fig. 5 Environmental dependence of FP coefficients for ETGs with $b/a > 0.6$. Symbols are the same as in Fig. 3.

dependence of coefficients a and b rather than weakening the dependence. Therefore, the bias on the surface brightness and the effective size would not affect our results.

4 DISCUSSION AND CONCLUSIONS

In this paper, we make use of the data from SDSS DR7 to study the environmental dependence of the FP relation for 70 793 ETGs. Due to the SDSS group catalog, for each galaxy we get the mass of its host dark matter halo, and specify it as a central or satellite galaxy in the halo. We investigate

Table 3 Fittings for our ETG Sample with Sky Background Correction

Band (1)	a (2)	b (3)	c (4)	$\mathrm{Scatter}_{\mathrm{orth}}$ (5)	$\mathrm{Scatter}_{R_0}$ (6)
g	1.340 ± 0.004	-0.737 ± 0.002	-8.55 ± 0.01	0.053	0.098
r	1.375 ± 0.004	-0.752 ± 0.002	-8.51 ± 0.01	0.052	0.096
i	1.392 ± 0.003	-0.768 ± 0.002	-8.55 ± 0.01	0.050	0.093
z	1.429 ± 0.003	-0.781 ± 0.002	-8.64 ± 0.01	0.049	0.093

Notes: FP fitting results of the ETG sample with sky background correction. Columns are similar to Table 1.

how FP coefficients depend on the halo mass and the position in the halo. We find the main results are as follows:

(1) The environmental dependence of the FP relation is similar in the g, r, i and z bands.
(2) FP coefficients of satellites are independent of their host halo mass and are close to those of the complete ETG sample.
(3) FP coefficients of centrals show significant dependence on the halo mass. We find b and c decrease but a increases with the halo mass. In small halos, the discrepancy between centrals and satellites is significant. In the largest halos, FP coefficients are similar to those of satellites.
(4) These relations still remain even when we only keep the red galaxies, or galaxies with $b/a > 0.6$, or galaxies with a radius in a specific range. Moreover, the sky background correction does not affect these results.

There are several studies on the correlation between FP coefficients and environmental density. D'Onofrio et al. (2008) studied the WIde-field Nearby Galaxy-cluster Survey (WINGS) sample, and found that in a denser environment a is larger but b and c are smaller. However, La Barbera et al. (2010b) combined SDSS and UKIDSS data and got a different result. They found that although the dependence of b and c is similar to D'Onofrio et al. (2008), a is smaller in the denser region. They explained that the discrepancy with D'Onofrio et al. (2008) might result from the fact that they corrected two biases of the FP slopes: one is due to the variation of averaged M/L from field to group galaxies, and the other is that the field and group have different distributions in the parameter space. Moreover, Magoulas et al. (2012) investigated about 10 000 ETGs in the 6dF Galaxy Survey. They found a and b are not dependent on the environment and c is smaller in the denser environment. All these studies found the global environmental dependence (cluster-centric distance, local galaxy density, etc.) of the FP is similar to the local environmental dependence (dark matter halo mass, group richness, etc.) but weaker.

All these studies did not distinguish between centrals and satellites as in this paper. For satellites, we did not find a correlation between FP coefficients and halo mass. For centrals, our findings are consistent with D'Onofrio et al. (2008), but conflict with the dependence of a in La Barbera et al. (2010b). Because La Barbera et al. (2010b) did two corrections, and because the correlation between a and the global environmental parameters is only significant at about 2σ, this is not a severe conflict.

As mentioned above, the tilt of the FP is the result of the non-constant M/L. This is due to non-homology and/or variations in stellar populations. One example of non-homology is the density profile of the dark matter halo. Centrals live in the center of the halo, where the dark matter density is higher and more sensitive to the halo mass than where satellites live. This may be one explanation for the environmental dependence found in this work. Moreover, when fitting the FP, luminosity L rather than stellar mass M_* is used. This introduces the contribution of stellar population (such as M_*/L or color) into the FP. Indeed, we find the environmental dependence of color is different for centrals and satellites. The color of centrals is redder in larger halos, but the color of satellites only weakly depends on the halo mass. Hyde & Bernardi (2009) indicated color can be treated as a fourth parameter to describe the FP. To explore these possibilities, the environmental dependence

of the stellar mass FP should be investigated. In the future, we will come back to this and study the contribution of stellar population to the variation in FP coefficients.

The distinction between the trends of centrals and satellites on the halo mass demonstrates that the dark matter halo affects centrals and satellites in different ways. Indeed, several studies found the quenching process satellites undergo is remarkably different from centrals. Peng et al. (2012) found the fraction of quenched centrals depends on the halo mass, but the quenched faction and the star formation rate (SFR) of satellites are mainly driven by the local density and further, are independent of the halo mass. Wetzel et al. (2013) demonstrated the SFR of centrals in larger halos peaks at a larger redshift; for satellites, the process of star formation evolved similarly to centrals before they fell into the main halo; afterward it is rapidly quenched in 0.2–0.8 Gyr; this quenching timescale is independent of the halo mass. Moster et al. (2013) also investigated this issue and concluded the SFR of centrals depends on the halo mass, and the stellar mass of satellites is determined by the mass of its subhalo when it is falling into the main halo.

All these studies suggest the quenching process of centrals is mainly determined by the halo mass, that is, the global environment, but the quenching of satellites depends on the local environment, which is little correlated with the mass of the main halo. This is consistent with results in this paper. Furthermore, the local density of the center of a halo is correlated with the halo mass. That means the quenching process of centrals depends on both the global and local environment, but satellites are only correlated with the local environment. This explains why the global environmental dependence of the FP is weaker than the local environmental dependence. In conclusion, the distinguishability between the environmental dependence of the FP relation for centrals and satellites may be driven by their different quenching processes.

Acknowledgements We are grateful to Xiaohu Yang for providing the SDSS group catalog. WY would like to acknowledge the support of the Fundamental Research Funds for Central Universities.

Funding for the SDSS and SDSS-II has been provided by the Alfred P. Sloan Foundation, the Participating Institutions, the National Science Foundation, the U.S. Department of Energy, the National Aeronautics and Space Administration, the Japanese Monbukagakusho, the Max Planck Society, and the Higher Education Funding Council for England. The SDSS Web Site is *http://www.sdss.org/*. The SDSS is managed by the Astrophysical Research Consortium for the Participating Institutions. The Participating Institutions are the American Museum of Natural History, Astrophysical Institute Potsdam, the University of Basel, Cambridge University, Case Western Reserve University, University of Chicago, Drexel University, Fermilab, the Institute for Advanced Study, the Japan Participation Group, Johns Hopkins University, the Joint Institute for Nuclear Astrophysics, the Kavli Institute for Particle Astrophysics and Cosmology, the Korean Scientist Group, the Chinese Academy of Sciences (LAMOST), Los Alamos National Laboratory, the Max-Planck-Institute for Astronomy (MPIA), the Max-Planck-Institute for Astrophysics (MPA), New Mexico State University, Ohio State University, the University of Pittsburgh, the University of Portsmouth, Princeton University, the United States Naval Observatory, and the University of Washington.

References

Aihara, H., Allende Prieto, C., An, D., et al. 2011, ApJS, 193, 29
Bernardi, M., Sheth, R. K., Annis, J., et al. 2003a, AJ, 125, 1817
Bernardi, M., Sheth, R. K., Annis, J., et al. 2003b, AJ, 125, 1849
Bernardi, M., Sheth, R. K., Annis, J., et al. 2003c, AJ, 125, 1866
Bernardi, M., Nichol, R. C., Sheth, R. K., Miller, C. J., & Brinkmann, J. 2006, AJ, 131, 1288
Bernardi, M., Hyde, J. B., Sheth, R. K., Miller, C. J., & Nichol, R. C. 2007, AJ, 133, 1741
Bernardi, M., Meert, A., Vikram, V., et al. 2014, MNRAS, 443, 874

Blanton, M. R., & Roweis, S. 2007, AJ, 133, 734
Bolton, A. S., Burles, S., Treu, T., Koopmans, L. V. E., & Moustakas, L. A. 2007, ApJ, 665, L105
Bolton, A. S., Treu, T., Koopmans, L. V. E., et al. 2008, ApJ, 684, 248
Bruce, V. A., Dunlop, J. S., Cirasuolo, M., et al. 2012, MNRAS, 427, 1666
Cappellari, M., Bacon, R., Bureau, M., et al. 2006, MNRAS, 366, 1126
Cappellari, M., Scott, N., Alatalo, K., et al. 2013, MNRAS, 432, 1709
Cimatti, A., Cassata, P., Pozzetti, L., et al. 2008, A&A, 482, 21
de Carvalho, R. R., & Djorgovski, S. 1992, ApJ, 389, L49
Djorgovski, S., & Davis, M. 1987, ApJ, 313, 59
D'Onofrio, M., Fasano, G., Varela, J., et al. 2008, ApJ, 685, 875
D'Onofrio, M., Fasano, G., Moretti, A., et al. 2013, MNRAS, 435, 45
Dressler, A., Lynden-Bell, D., Burstein, D., et al. 1987, ApJ, 313, 42
Faber, S. M., & Jackson, R. E. 1976, ApJ, 204, 668
Graves, G. J. 2009, in Galaxy Evolution: Emerging Insights and Future Challenges, Astronomical Society of the Pacific Conference Series, 419, eds. S. Jogee, I. Marinova, L. Hao, & G. A. Blanc, 96
He, Y. Q., Xia, X. Y., Hao, C. N., et al. 2013, ApJ, 773, 37
Hyde, J. B., & Bernardi, M. 2009, MNRAS, 396, 1171
Jing, Y. P., Mo, H. J., & Börner, G. 1998, ApJ, 494, 1
Jorgensen, I., Franx, M., & Kjaergaard, P. 1995, MNRAS, 276, 1341
Jorgensen, I., Franx, M., & Kjaergaard, P. 1996, MNRAS, 280, 167
Koopmans, L. V. E., Treu, T., Bolton, A. S., Burles, S., & Moustakas, L. A. 2006, ApJ, 649, 599
La Barbera, F., de Carvalho, R. R., de La Rosa, I. G., & Lopes, P. A. A. 2010a, MNRAS, 408, 1335
La Barbera, F., Lopes, P. A. A., de Carvalho, R. R., de La Rosa, I. G., & Berlind, A. A. 2010b, MNRAS, 408, 1361
Lauer, T. R., Faber, S. M., Richstone, D., et al. 2007, ApJ, 662, 808
Lucey, J. R., Bower, R. G., & Ellis, R. S. 1991, MNRAS, 249, 755
Magoulas, C., Springob, C. M., Colless, M., et al. 2012, MNRAS, 427, 245
Moster, B. P., Naab, T., & White, S. D. M. 2013, MNRAS, 428, 3121
Nigoche-Netro, A., Ruelas-Mayorga, A., & Franco-Balderas, A. 2009, MNRAS, 392, 1060
Peacock, J. A., & Smith, R. E. 2000, MNRAS, 318, 1144
Peng, Y.-j., Lilly, S. J., Renzini, A., & Carollo, M. 2012, ApJ, 757, 4
Reda, F. M., Forbes, D. A., & Hau, G. K. T. 2005, MNRAS, 360, 693
Rusin, D., & Kochanek, C. S. 2005, ApJ, 623, 666
Springob, C. M., Magoulas, C., Proctor, R., et al. 2012, MNRAS, 420, 2773
Treu, T., Koopmans, L. V., Bolton, A. S., Burles, S., & Moustakas, L. A. 2006, ApJ, 640, 662
Treu, T., & Koopmans, L. V. E. 2004, ApJ, 611, 739
Trujillo, I., Burkert, A., & Bell, E. F. 2004, ApJ, 600, L39
Trujillo, I., Feulner, G., Goranova, Y., et al. 2006, MNRAS, 373, L36
Tully, R. B., & Fisher, J. R. 1977, A&A, 54, 661
van den Bosch, F. C., Aquino, D., Yang, X., et al. 2008, MNRAS, 387, 79
van Dokkum, P. G., Franx, M., Kriek, M., et al. 2008, ApJ, 677, L5
von der Linden, A., Best, P. N., Kauffmann, G., & White, S. D. M. 2007, MNRAS, 379, 867
Wegner, G., Colless, M., Saglia, R. P., et al. 1999, MNRAS, 305, 259
Weinmann, S. M., van den Bosch, F. C., Yang, X., & Mo, H. J. 2006, MNRAS, 366, 2
Wetzel, A. R., Tinker, J. L., Conroy, C., & van den Bosch, F. C. 2013, MNRAS, 432, 336
Woo, J., Dekel, A., Faber, S. M., et al. 2013, MNRAS, 428, 3306
Yang, X., Mo, H. J., & van den Bosch, F. C. 2003, MNRAS, 339, 1057
Yang, X., Mo, H. J., van den Bosch, F. C., & Jing, Y. P. 2005, MNRAS, 356, 1293
Yang, X., Mo, H. J., van den Bosch, F. C., et al. 2007, ApJ, 671, 153
Yang, X., Mo, H. J., van den Bosch, F. C., Zhang, Y., & Han, J. 2012, ApJ, 752, 41